J. King Saud Univ., Vol. **3**, *Eng. Sci.* (1), pp. 69–87 (1411H/1991)

Prediction of Drying Shrinkage of Portland Cement Paste: Influence of Shrinkage Mechanisms

Jamal A. Almudaiheem
Assistant Professor, Civil Engineering Department, College of Engineering, King Saud University, P.O. Box 800, Riyadh 11421, Saudi Arabia

Abstract. Ultimate drying shrinkage of paste was investigated in terms of the Gibbs-Bangham shrinkage and the capillary stress mechanisms. Shrinkage measurements and nitrogen sorption isotherms were obtained on cement pastes of water-to-cement (W/C) ratios of 0.4, 0.6 and 0.75. The contribution to ultimate drying shrinkage from these two mechanisms was obtained from ultimate shrinkage versus increase in surface free energy curves in the relative humidity (RH) range of 95 to 0 percent. The Gibbs-Bangham stress mechanism is the major contributor to shrinkage stresses in this RH range. The capillary stress mechanism is active in the RH range of 95 to 50 percent.

The maximum Gibbs-Bangham stress shrinkage, which occurs at 0 percent RH, is linearly proportional to total surface area as obtained from volume-thickness (V-t) sorption analysis. Maximum capillary stress shrinkage occurs at about 50 percent RH. This component was found to be linearly proportional to cumulative capillary surface area. V-t adsorption analysis was used to estimate the cumulative capillary surface area. The equations for predicting maximum Gibbs-Bangham and capillary stress shrinkage were extended to include effect of RH of drying. They were tested on different shrinkage results of well-hydrated pastes of 0.4 and 0.6 W/C ratios and found to be accurate.

Introduction

Drying shrinkage of concrete is a property of the microstructure of the hydrated cement paste and the strong interaction between the hydrophilic surface and water [1,2]. Drying process involves removal of water which in turn creates substantial stresses. These stresses become significant in high surface area systems such as cement paste.

Four shrinkage mechanisms have been proposed to explain the drying shrinkage phenomena of porous materials. They are: change in surface free energy (Gibbs-Bangham effect) of the solid phase due to sorption of water vapor [3-9], capillary tension effect due to meniscus formation in the capillary pores which results in equal

hydrostatic compression in the solid phase [3,4,9-12], changes in the disjoining pressure in areas of hindered adsorption [3,4,8,13,14]; and movement of interlayer water [5-8,10,12,14]. The contribution to overall shrinkage from the individual shrinkage mechanism is unclear. It is well known that opinions differ widely about the role of the four mechanisms in causing the shrinkage. There seems to be an agreement between different researchers that most of the shrinkage occurring upon drying at RH higher than 40 percent is caused by capillary tension mechanism [3-6,8,15]. Whereas, shrinkage is mainly caused by changes in surface energy of the gel particle upon drying at RH lower than 40 percent [3,4,8,15].

In the present study the feasibility of predicting drying shrinkage of paste in terms of the predominant two mechanisms (namely the Gibbs-Bangham and Capillary tension) will be investigated. A wide range in pore structure variations will be obtained by varying the W/C ratio and curing time.

Materials and Methods

A commercial Type I portland cement was used. All mixing and curing operations were performed at a room temperature of 23 ± 2°C (74 ± 3°F). The water to cement (W/C) ratios used were 0.4, 0.6 and 0.75. The pastes were hand mixed for two minutes then rotated in sealed containers at 10 rpm before casting to minimize sedimentation and bleeding. The pastes were cast in plexiglass molds after they reached suitable consistency and rotated for 24 hours. The slabs were demolded and cured until time of test in air-tight containers filled with lime-saturated water. At the end of the curing period, thin specimens measuring 2.5 × 10 × 75 mm (0.1 × 0.4 × 3 in.) were cut from the slabs using a diamond saw.

A stainless steel clamp was mechanically attached to each specimen end to facilitate shrinkage measurements. The clamp has a spherical slot at its center for accurate sitting on the steel spheres attached to each measuring end in the dial gauge. The dial gauge was constructed by Dr. L.J. Parrott (from Cement and Concrete Association, London) to Dr. W. Hansen [16]. The reproductibility of the dial gauge reading was within ± 5 microstrain. Drifts in readings were compensated for by using an invar stainless steel bar. The specimens were dried in desiccators conditioned at 90, 75, 60, 50, 30, 11 and 0 percent RH. The RH levels were obtained using aqueous solution of sulfuric acid. The zero percent RH corresponds to the vapor pressure above concentrated sulfuric acid. The RH was maintained constant in each desiccator by stirring the solution continuously during the entire drying period. The concentration of the sulfuric acid solution in each desiccator was monitored with time to ensure that the RH is constant. The desiccators were kept in an environmental chamber where the temperature was maintained at 23 ± 1°C (74 ± 1°F).

Specimens used for pore structure measurements were solvent replaced with methanol for at least 3 weeks. The methanol was changed several times during this

period. Solvent replacement is a widely accepted and recommended technique for pore structure measurements using Nitrogen Sorption Isotherm or Merury Intrusion Porosimetry. The solvent replacement technique was used in order to protect the original pore structure from extensive pore collapse on drying [17]. This technique was used with the entire specimens. Therefore, if there were any effect from the interaction between the methanol with the C-S-H surfaces, as claimed by some researchers [18], the effect would be relative and the findings will hold true. This is supported by Parrott [19]. About 50 to 100 mg of each specimen was crushed into pieces of 2.5 mm thickness and dried at 0 percent RH for at least one week before pore structure measurement using nitrogen sorption.

The dynamic flow method was used to obtain the nitrogen sorption isotherms*. The carrier gas was helium. Desorption and adsorption curves were obtained in the relative vapor pressure (P/P_0) region of about 0.98 to about 0.05. For V-t analysis the reference t curve by Cranston and Inkley [20] was used.

Shrinkage and pore structure results of different pastes of 0.4 and 0.6 W/C ratios cured for 165 days were used as well as in the present study to validate the proposed approach.

Theoretical Background

Gibbs-Bangham Shrinkage Stress

The changes in surface free energy with relative humidity are described by the Gibbs free energy equation:

$$\triangle\gamma = \frac{10^{-7} \times RT}{\overline{V}} \int_{P_1/P_0}^{P_2/P_0} \frac{V_a}{S_s} \, d \ln \frac{P}{P_0} \qquad (1)$$

where $\triangle\gamma$ is the calculated increase in surface free energy in N/m, R is the gas constant (dyne.cm/mol.K), T is the absolute temperature in degrees Kelvin, $\overline{V}$ is the molar volume of adsorbed liquid (cm^3/mole), V_a is the volume of adsorbed liquid (cm^3/g dry), S_s is the specific surface area (m^2/g. dry), and P/P_0 is the relative vapor pressure.

Bangham and his co-workers [21,22] proposed the following empirical equation which relates the expansion (ε_{exp}) of highly porous material (charcoal) and the changes in surface free energy ($\triangle\gamma$):

$$\varepsilon_{exp} = \lambda \triangle\gamma \qquad (2)$$

where λ is a material constant. Amberg and MacIntoch [23] confirmed the linear relationship between the expansion of Vycor glass and the decrease in surface free energy upon adsorption of water.

* Quantasorb, Quantachrome Co., six aerial way, Syosset, New York

Bangham and Maggs [24] have related λ to the elastic modulus of a high surface area solid (E_s) by the following expression:

$$\lambda = \frac{S_s \varrho_s}{E_s} \tag{3}$$

where ϱ_s is the solid density. Different expressions have been proposed by Hiller [25] and Yates [26]. They differ only from the expression by Bangham and Maggs by a proportionality factor. Thus, in general:

$$\varepsilon_{exp} = KS_s \tag{4}$$

where K is constant.

Capillary Shrinkage Stresses

Menisci are formed in capillary pores upon drying. The menisci create hydrostatic tension in the remaining water which is transferred to the solid pore walls as hydrostatic compressive stresses (P_{cap}). These stresses increase with decreasing pore size as predicted by the Laplace equation:

$$P_{cap} = \frac{2 \gamma_\omega}{r} \tag{5}$$

where r is the radius of curvature of the meniscus assuming a hemispherical surface, and γ_ω is the water density.

The relationship between the radius of curvature and vapor pressure (P/P_0) can be obtained from the Kelvin equation where:

$$\ln \frac{P}{P_0} = \frac{2 \gamma_\omega \overline{V}}{R T r} \tag{6}$$

combining equations 5 and 6 it can be shown that

$$P_{cap} = K_1 \ln \frac{P}{P_0} \tag{7}$$

where K_1 is a material constant.

No fundamental relationship has been developed between capillary stresses and shrinkage (ε_{cap}) of Portland cement paste. This may be attributed to the complixity of the pore system. In general, one would expect that

$$\varepsilon_{cap} = f(P_s, P_g, E_s) P_{cap} \tag{8}$$

where $f(P_s, P_g, E_s)$ is a function of the pore structure, pore geometry, and elastic modulus of the solid. From equations 7 and 8 it follows that:

$$\varepsilon_{cap} = K_1 f(P_s, P_g, E_s) \ln\frac{P}{P_0} \quad (9)$$

Thus, a relationship between $\ln\frac{P}{P_0}$ and capillary stress shrinkage may be empirically obtained.

Results and Discussion

Ultimate Drying Shrinkage of Paste Versus Relative Humidity of Drying, as Influenced by W/C Ratio and Curing Time

Figure 1 illustrates the development of drying shrinkage over drying time at 90, 75, 60, 50, 30, 11 and 0 percent RH for the 0.6 W/C ratio paste cured 30 days. Each point on the shrinkage curves is the average of two companion specimens. The variations in shrinkage between companion specimens were within 0.02 percent. The curves are similar to the other paste systems investigated. The shape of the shrinkage curves is in general agreement with those reported by other investigators [27-29].

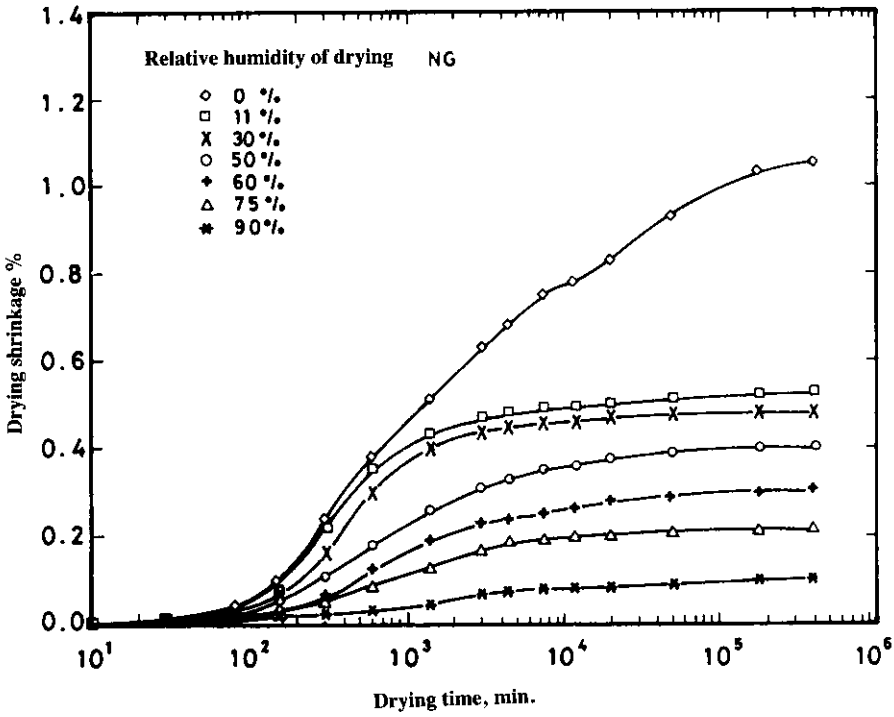

Fig. 1. Development of drying shrinkage over time curves for thin paste specimens of 0.6 W/C ratio hydrated 30 days.

The results illustrate that ultimate drying shrinkage is not reached within the drying period of 275 days. However, these values were assumed to be ultimate since the additional shrinkage extrapolated out to several years is insignificant. Ultimate drying shrinkage values for the paste systems investigated are shown in Table 1.

Table 1. Ultimate drying shrinkage (%) versus RH of drying for the paste systems investigated

W/C ratio	Length of curing (days)	Percent of relative humidity						
		90	75	60	50	30	11	0
0.4	3	0.07	0.17	0.24	0.28	0.34	0.40	0.79
	30	0.06	0.16	0.25	0.34	0.41	0.49	0.91
	240	0.04	0.13	0.25	0.32	0.40	0.46	1.00
0.6	7	0.07	0.17	0.22	0.26	0.33	0.39	0.80
	30	0.10	0.20	0.30	0.40	0.48	0.52	1.04
	240	0.07	0.18	0.29	0.41	0.47	0.55	1.10
0.75	9	0.05	0.17	0.25	0.30	0.38	0.51	0.89
	30	0.08	0.22	0.30	0.39	0.47	0.54	1.08
	240	0.05	0.20	0.32	0.47	0.56	0.61	1.04

Contribution to Ultimate Shrinkage from the Two Stress Active Shrinkage Mechanisms

Two stress active shrinkage mechanisms may be interpreted from the curves of ultimate drying shrinkage versus calculated increase in surface free energy shown in Fig. 2. The major shrinkage contributor illustrated by the dotted lines is due to the Gibbs- Bangham stress mechanism since it follows equation (2). This mechanism is active over the entire RH range between 95 and 0 percent. The systems shown are pastes of 0.4, 0.6, and 0.75 W/C ratio cured for 30 days. The curves are typical for the systems investigated, and are in good agreement with those reported by Amberg and MacIntoch [23] on porous Vycor glass.

The sorption isotherms and the V-t curves are shown in Figs 3a, 3b, 3c and Figs. 3d, 3e, 3f, respectively. The V-t curves were constructed from nitrogen sorption isotherms and the reference t curve of Cranston and Inkley [20]. The increase in surface free energy versus RH was calculated from equation (1). The relationship between volume of liquid adsorbed normalized for surface area (V_a/S) versus ln P/P_0 was estimated from V-t adsorption curves corrected for capillary condensation volume. It was found that, the relationship between (V_a/S) versus ln P/P_0 is similar for the paste systems investigated. Therefore, the calculated increase in surface free energy versus RH is similar for these systems. The results are shown in Table 2.

Ninety-five percent RH was the starting point for estimating the increase in surface free energy with decrease in RH due to the uncertainty in obtaining (V_a/S) at t values greater than 1.6 nm. Further, it is assumed that zero drying shrinkage has occurred between 100 and 95 percent RH. A zero percent RH in the calculations corresponds to a value of –7.5 in ln P/P_0.

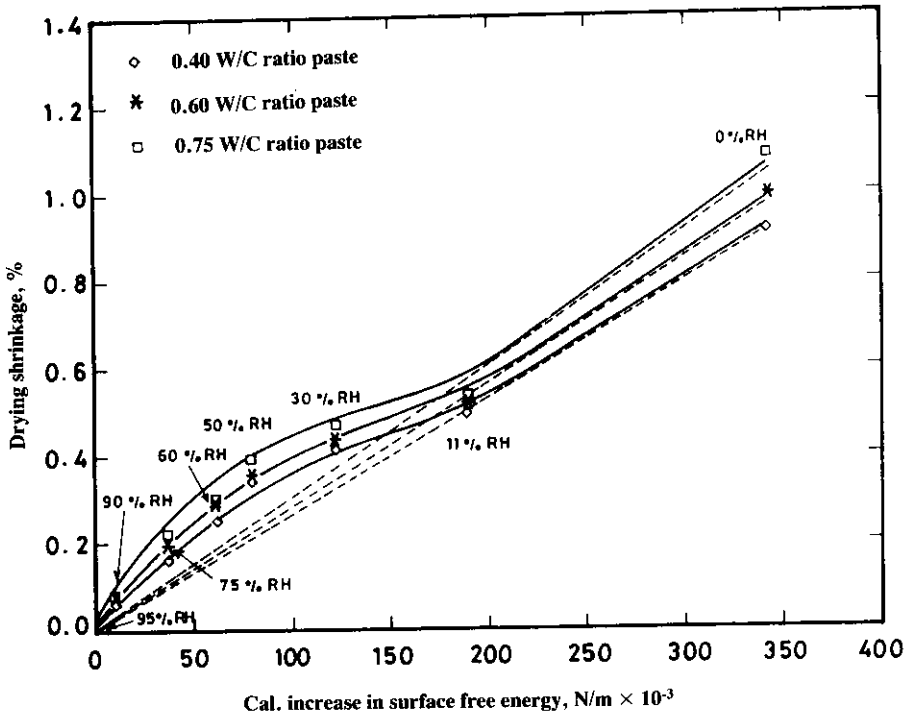

Fig. 2. Drying shrinkage versus increase in surface free energy curves obtained for thin paste specimens of 0.4, 0.6 and 0.75 W/C ratio hydrated 30 days.

Table 2. Calculated increase in surface free energy for incremental RH steps

RH %	$\Delta\gamma$ ($\times 10^{-3}$ N/m)	$\Sigma\Delta\gamma$ ($\times 10^{-3}$ N/m)
90-95	10.1	10.1
75-90	26.4	36.5
60-75	24.8	61.3
50-60	17.7	90.0
30-50	43.2	122.2
11-30	66.8	189.0
0-11	152.6	341.6

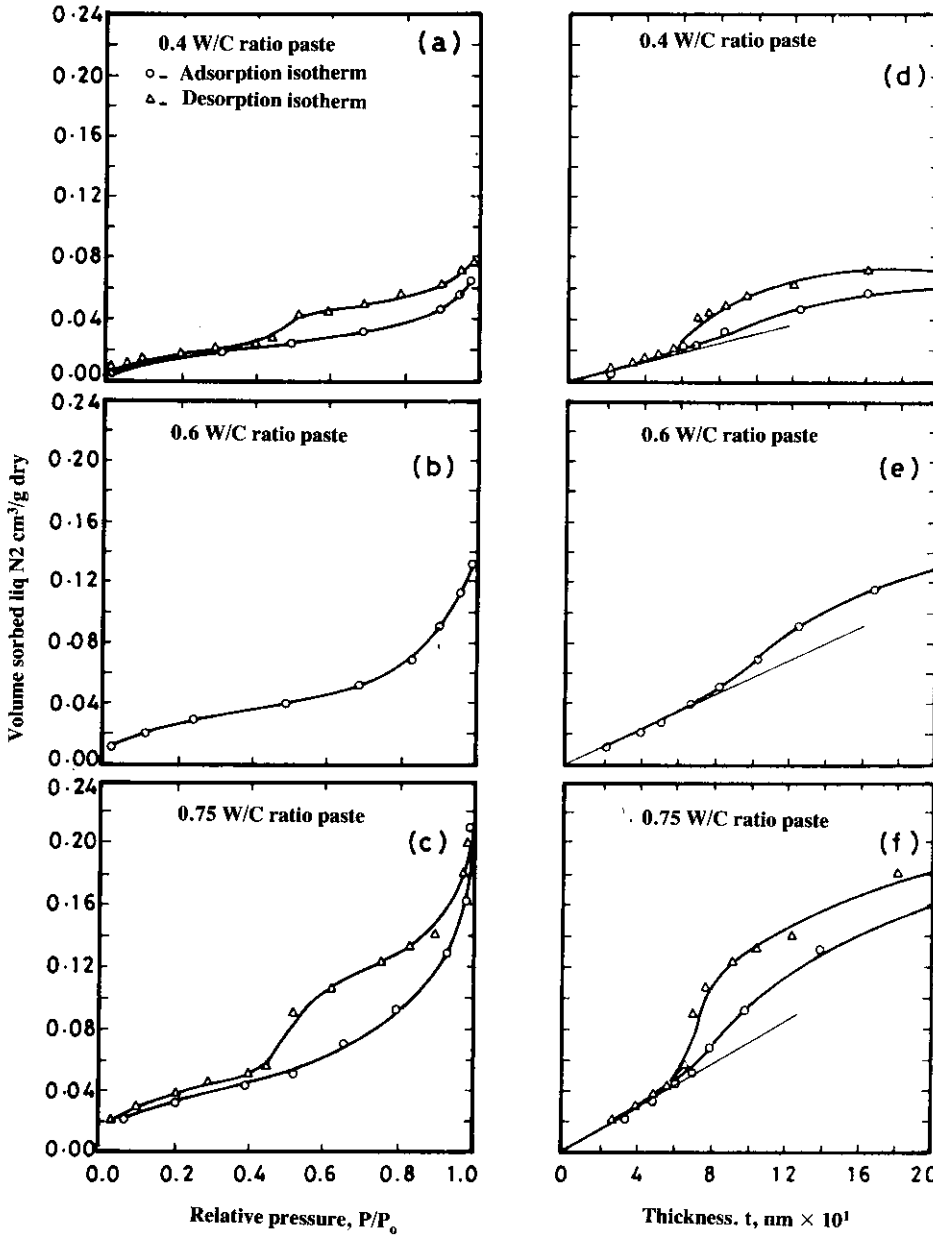

Fig. 3. Nitrogen isotherms and V-t curves of 0.4, 0.6 and 0.75 W/C ratio pastes hydrated for 30 days. Solvent replaced in methanol for 3 weeks before drying at 0% RH.

In Fig. 2 capillary stress shrinkage is the component superimposed onto the Gibbs-Bangham stress shrinkage in the RH range between 95 and about 50 percent. This is supported by nitrogen V-t curves in Figs 3d, 3e, and 3f which show capillary condensation in the t value range of about 0.68 to 1.1 nm. This corresponds to an RH range of about 50 to 85 percent RH. The capillary stress shrinkage at about 50 percent RH is about 50 to 60 percent of the Gibbs-Bangham stress shrinkage. Further, the capillary condensation volume below about 50 percent RH is insignificant. Consequently, capillary stress shrinkage is insignificant below 50 percent RH.

The results in Fig. 2 suggest that capillary stress shrinkage is entirely irreversible since it increases gradually from 95 percent to its maximum value near 50 percent RH for each of the three systems investigated. The capillary stresses, however, are not cumulative. The irreversible nature of capillary stress shrinkages agrees well with results by other investigators [3,10,30,31].

Figs 4a, 4b, and 4c show capillary stress shrinkage versus RH of drying curves of the 0.4, 0.6 and 0.75 W/C ratio pastes and the influence curing time. These curves were constructed from ultimate shrinkage versus increase in surface free energy curves such as those shown in Fig. 2. For the 0.6, and 0.75 W/C ratio pastes capillary stress shrinkage at 50 percent RH increases with curing time. It is unaffected by curing time in the 0.4 W/C ratio paste. Figs 4a, 4b, and 4c show that the capillary stress shrinkage increases with increasing W/C ratio.

Shrinkage stresses below 50 percent RH may be entirely due to Gibbs-Bangham stress. However, the additional shrinkage between 50 and 11 percent RH is only a fraction of the Gibbs-Bangham stress shrinkage predicted by the dotted lines in Fig. 2. This transition range occurs due to a drop in the total stresses caused by the disappearance of capillary stresses. Below 11 percent RH the shrinkage versus increase in surface free energy relationship will again follow that described by the dotted line. The occurrence of the transition range suggests that, a major part of first drying shrinkage is inelastic decrease of interlayer spaces and that true Gibbs-Bangham shrinkage is only a fraction of total shrinkage. Further, shrinkage in this range is nearly linear with increase in surface free energy. Table 3 illustrates that the additional shrinkage between 50 and 11 percent RH is approximately 52 percent of the original Gibbs-Bangham stress shrinkage in this RH range as predicted by the dotted line.

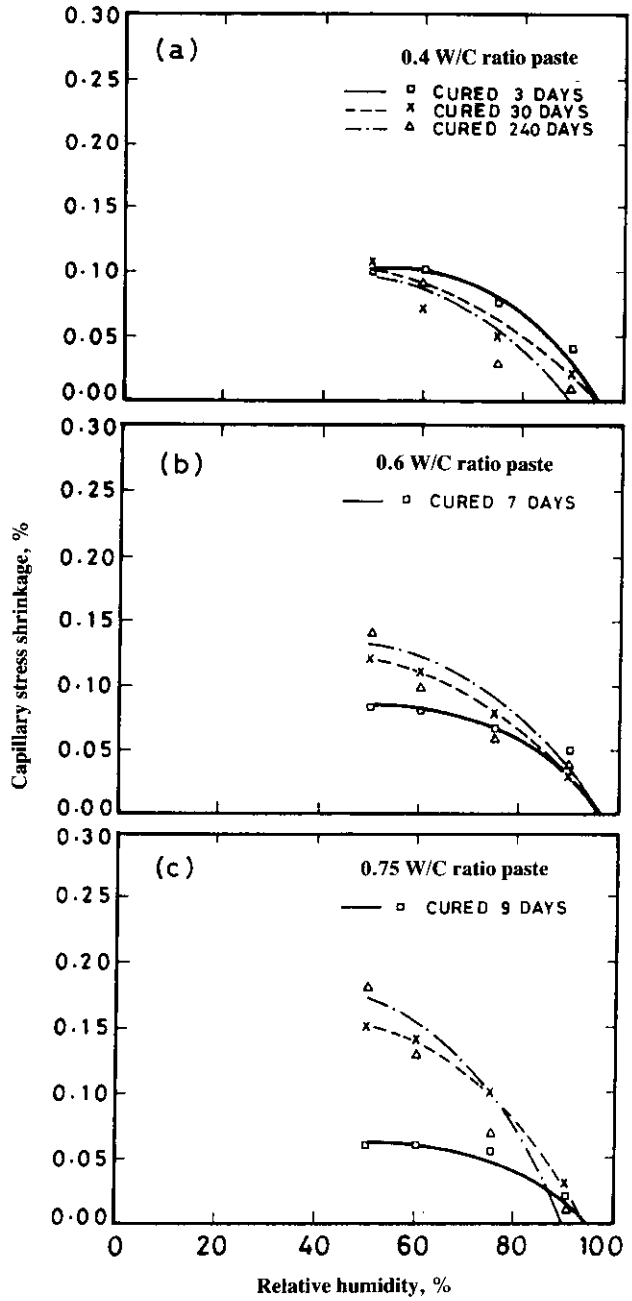

Fig. 4. Capillary stress shrinkage versus relative humidity curves for 0.4, 0.6 and 0.75 W/C ratio Portland cement pastes.

Table 3. Shrinkage between 50 and 11 percent RH as fraction of Gibbs-Bangham stress shrinkage

W/C	Cured, days	Shrinkage ratio (percent)
0.4	3	48
	30	48
	240	51
0.6	7	64
	30	50
	240	40
0.75	9	72
	30	51
	240	40

Effect of Nitrogen Surface Area and RH of Drying on Gibbs-Bangham and Capillary Stress Shrinkage

Maximum Gibbs-Bangham stress shrinkage versus total surface area and capillary stress shrinkage versus capillary surface area are shown in Figs 5 and 6 respectively for the pastes investigated. Shrinkage values were obtained from ultimate shrinkage versus increase in surface free energy curves whereas surface areas were estimated from nitrogen V-t curves. The total surface areas were obtained from the slopes of the initial straight line portions of the V-t curves. The capillary surface areas were calculated from the V-t adsorption curves. Assuming cylindrical pore shape, the pore diameter range in which condensation occurred upon adsorption was about 4 to 20 nm. The capillary surface areas for pores larger than about 20 nm was estimated from the slope of the V-t adsorption curve at a t-value of 2 nm. This t-value was used in order to avoid effects of micropore filling. Incorporating the capillary surface area of pores larger than 20 nm is justified since a substantial amount of capillary stress shrinkage occurs between 90 and 95% RH as seen in Figs 4a, 4b, 4c. This corresponds to capillary pore diameter between about 20 and 40 nm respectively. Table 4 illustrates that micropores are present in all the paste investigated since the total surface area values are substantially larger than those calculated for the capillaries. Further, the micropores are larger in width than 1.6 nm since no downward deviation in the V-t curves occurs at t-values smaller than 0.8 nm. Linear regression of the results in Figs 5 and 6 yields the following two equations:

$$\varepsilon_{GB}\,(0\%\mathrm{RH}) = 0.655 + 0.00524S_{tot} \tag{10}$$

and,

$$\varepsilon_{cap}\,(50\%) = 0.01524 + 0.00251S_{cap} \tag{11}$$

Table 4. Nitrogen surface areas of the pastes studies

W/C ratio	Curing length (days)	S_{tot} m^2/g dry	S_{cap} m^2/g dry
0.40	7	30	17
	30	34	17
	240	45	22
0.60	7	49	34
	30	60	39
	240	84	54
0.75	9	35	26
	30	72	49
	240	96	62

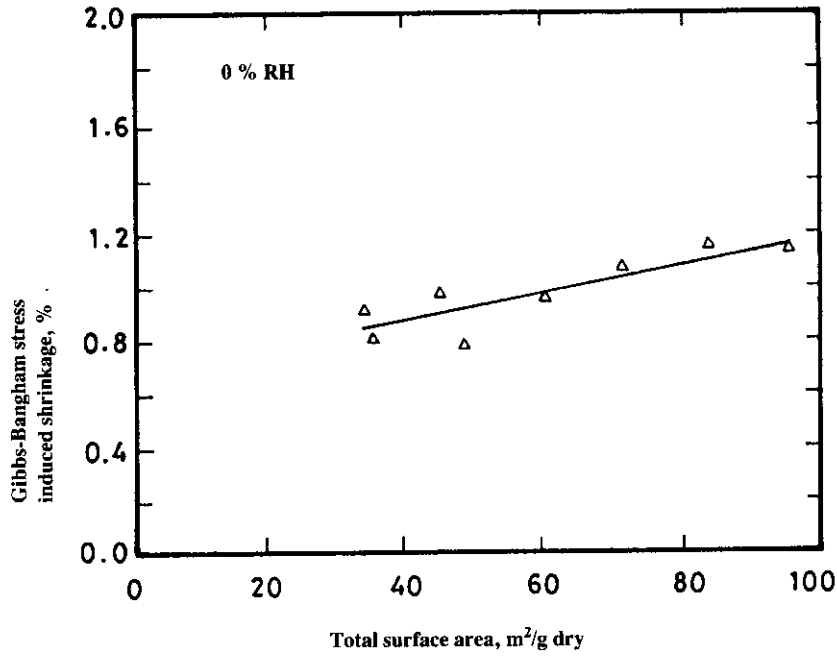

Fig. 5. Gibbs-Bangham stress shrinkage at 0 % RH versus total surface area

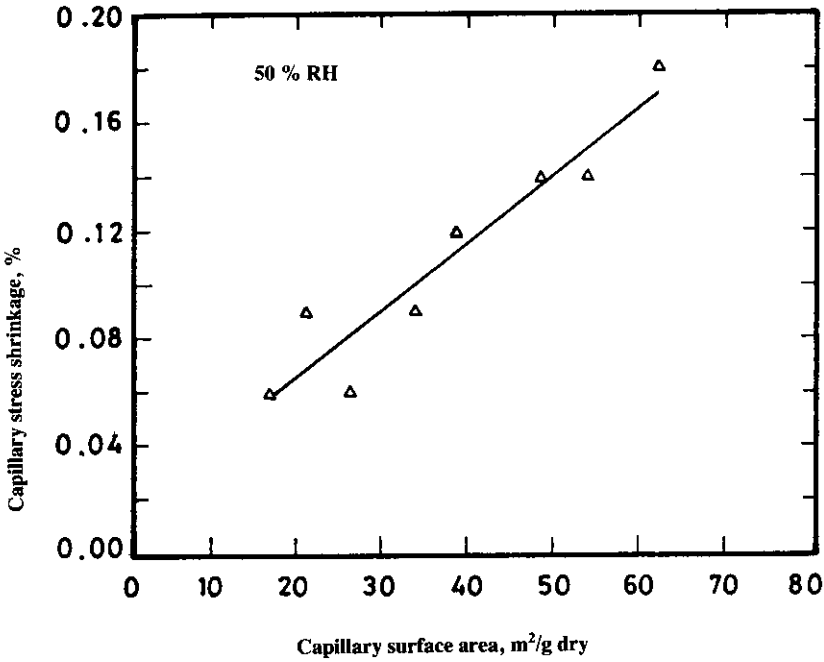

Fig. 6. Capillary stress shrinkage at 50 % RH versus capillary surface area

Where $\varepsilon_{GB}(0\%RH)$ is the Gibbs-Bangham stress shrinkage at zero percent RH, and ε_{cap} (50%RH) is the capillary stress shrinkage at 50 percent RH. S_{tot} and S_{cap} are the total and capillary surface areas in m^2/g dry respectively. The surface areas were obtained from nitrogen sorption analysis. The correlation coefficients for equations (10) and (11) are 0.742 and 0.901 respectively.

The linear relationship between Gibbs-Bangham stress shrinkage and total surface area is in good agreement with theory (equation 4). The positive intercept with shrinkage at zero surface area is another indication that a major fraction of first drying shrinkage is due to a decrease in interlayer spacing. This is also consistent with the results in Fig. 6.

Equations (10) and (11) can be modified to include the effect of RH. Based on the results shown in Table 2 for the increase in surface free energy versus decrease in RH a linear relationship is obtained in the RH range of 95 to 20 percent. It is described by the following equation:

$$\Delta\gamma = 174.5 - 1.85RH \tag{12}$$

where

$$20\% \leqslant RH \leqslant 95\%$$

A correlation coefficient of 0.996 was obtained from the regression line in this RH range. The RH range below 20 percent has little practical importance, therefore, it is excluded in this study. The follwing equation is obtained by combining equations 10 and 12.

$$\varepsilon_{GB}(RH) = (0.264 + 0.00211S_{tot}) \left(\frac{174.5 - 1.85RH}{137.5} \right) \tag{13}$$

This equation is used to calculate the shrinkage component due to Gibbs-Bangham stress in the RH range of 95 to 50 percent. The shrinkage component due to capillary stresses in the RH range of 95 to 50 percent can be conveniently obtained from the following empirical relationship:

$$\varepsilon_{cap}(RH) = (0.015 + 0.0025\, S_{cap}) \left(\frac{\frac{\ln RH}{100}}{\ln 0.5} \right) \tag{14}$$

where

$$50\% \leq RH \leq 95\%$$

In the RH range of 95 to 50 percent total drying shrinkage, ε_t is obtained by superimposing the two shrinkage components. Thus:

$$\varepsilon_t(RH) = \varepsilon_{GB}(RH) + \varepsilon_{cap}(RH) \tag{15}$$

Between 50 and 11 percent RH the additional shrinkage, which is Gibbs-Bangham stress induced, is obtained from the following equation:

$$\varepsilon_{tr}(RH) = 0.52\, \varepsilon_{GB}(RH) \tag{16}$$

where ε_{tr} is the additional shrinkage in the transition range (*i.e.* 50 to 11 percent RH). Thus, total shrinkage (ε_t) between 50 to 11 percent RH is given by the following expression:

$$\varepsilon_t = \varepsilon_t(50\%) + \varepsilon_{tr}(RH) \tag{17}$$

Testing of the Proposed Equations for Predicting Drying Shrinkage of Paste in the RH Range of 95 to 20 percent

Excellent agreement between measured and predicted ultimate shrinkage of a 0.4 W/C ratio paste was obtained at any RH between 95 and 20 percent. This is shown in Fig. 7. For the 0.6 W/C ratio paste good agreement was obtained as seen in Fig. 8. For this paste, the predicted shrinkage values are slightly below those measured with a maximum deviation of about 20 percent at 75 percent RH. This deviation might be explained by the other two mechanisms. But, unfortunately, these two mechanisms can not be quantified by any mean.

Thus, the empirical equations developed in this study can be used to predict the ultimate drying shrinkage of pastes of different W/C ratios in the RH range between 95 and 20 percent. The total estimated surface area and cumulative capillary surface area values for the two paste systems used are shown in Table 5.

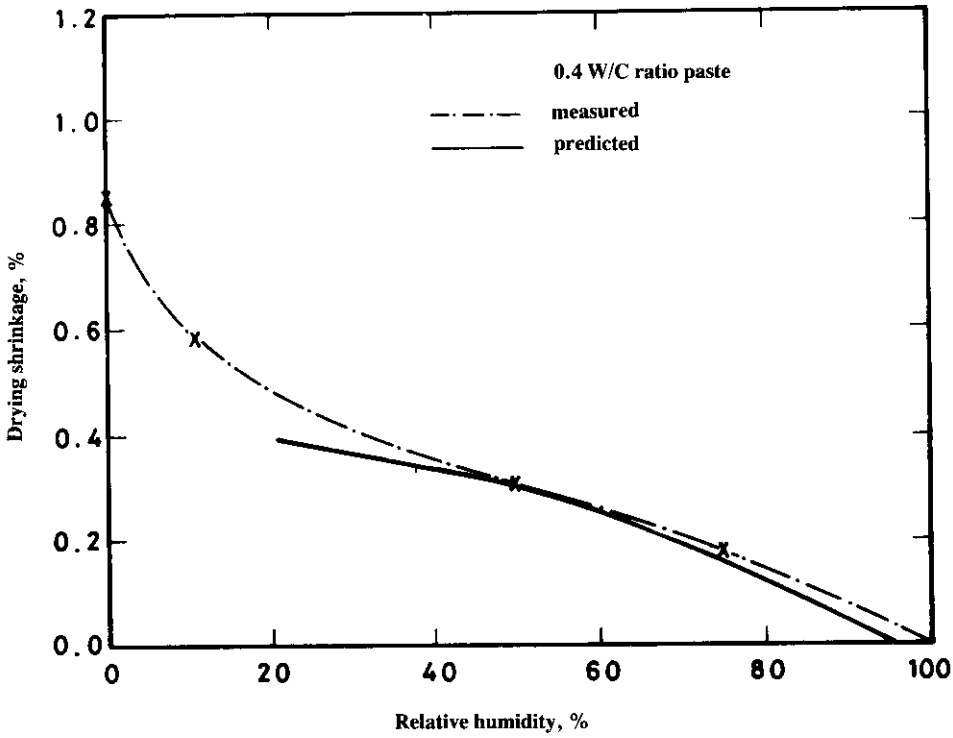

Fig. 7. Predicted and measured curves of drying shrinkage versus RH of Portland cement paste hydrated for 165 days

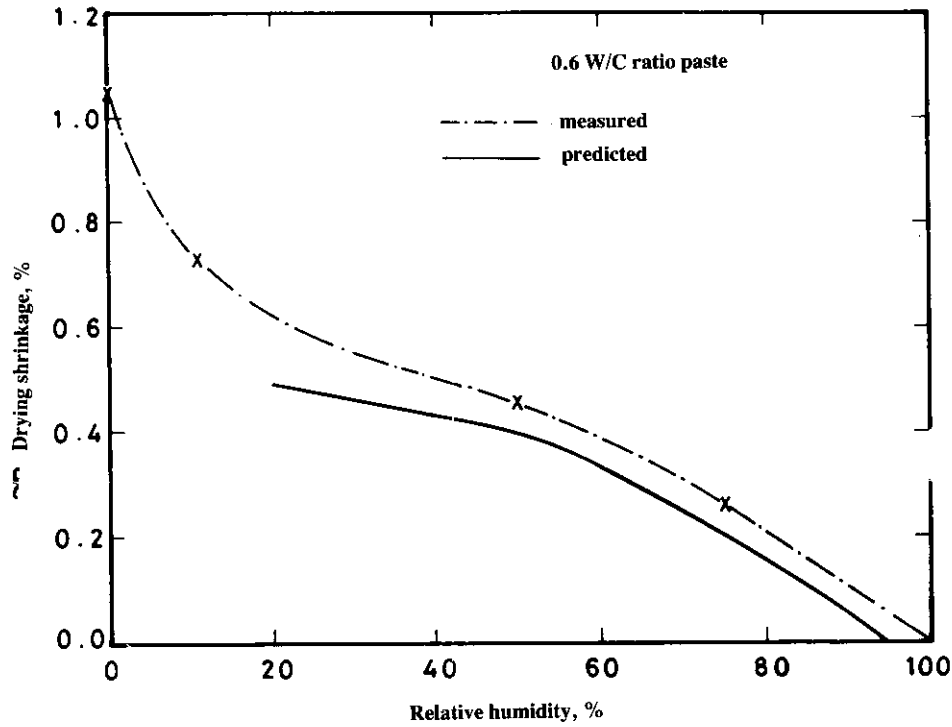

Fig. 8. Predicted and measured drying shrinkage versus RH curves of Portland cement paste hydrated for 165 days

Table 5. Surface area values for the 0.4 and 0.6 W/C ratio pastes

W/C	Length of curing (days)	Total surface area (m^2/g dry)	Capillary surface area (m^2/g dry)
0.40	165	53	27
0.60	165	83	50

Conclusions

The Gibbs-Bangham mechanism was found to be the major contributor to shrinkage stresses of cement paste in the entire RH range of 95 to 0 percent. The capillary stress mechanism was found to be active in the RH range of 95 to 50 percent. Its contribution to overall shrinkage increases with W/C ratio and is maximum at about 50 percent RH. The capillary stress shrinkage at 50 percent RH is about 50 to 60 percent of Gibbs-Bangham stress shrinkage.

The contribution of the two mechanisms to ultimate drying shrinkage versus RH can be obtained from shrinkage versus increase in surface free energy curves.

It was found that maximum Gibbs-Bangham stress shrinkage, which occurs at 0 percent RH, can be accurately predicted from an empirical relationship with total surface area as obtained from nitrogen V-t curves. The maximum capillary stress shrinkage, which occurs at 50 percent RH, can be accurately predicted from another empirical equation which incorporates the cumulative capillary surface area. The capillary surface area values were calculated from V-t adsorption curves. The shrinkage equations were extended to include effect of RH of drying in the RH range of 95 to 20 percent.

Shrinkage stresses below about 50 percent RH are mainly due to the Gibbs-Bangham mechanism. Drying shrinkage between about 50 and 11 percent RH is approximately 52 percent of the original Gibbs-Bangham shrinkage.

The proposed equations for predicting ultimate drying shrinkage of cement pastes were tested on shrinkage results of two different W/C ratio pasts. Overall agreement with shrinkage results was found to be good in the RH range tested. The differences between actual and predicted curves could be explained by the other two mechanisms if there were any means that they can be quantified.

References

[1] Verbeck, G. "Pore Structure." Significance of Tests and Properties of Concrete and Concrete Making Materials. *American Society for Testing and Materials,* Philadelphia, STP 169B, (1978), 262-271.

[2] Powers, T.C. and Brownyard, T.L. *ACI Journal Proceedings,* 43 (1947), 101, 249, 469, 549, 669, 845, 933.

[3] Powers, T.C. "Mechanisms of Shrinkage and Reversible Creep of Hardened Cement Paste." *Proc. Intern. Conf. Struct. Conc.* London (1965), 319-334.

[4] Powers, T.C. "The Thermodynamics of Volume Change and Creep." *Mater. Struct.,* 1, No. 6 (1968), 487-507.

[5] Feldman, R.F. "Sorption and Length Change Scanning Isotherms of Methanol and Water of Hydrated Portland Cement." *Proc. 5th Intl. Symp. Chem. Cem.,* Tokyo, Part III (1968), 53-66.

[6] Feldman, R.F. and Sereda, P.J. "Sorption of Water on Compacts of Bottle-Hydrated Cement, 2. Thermodynamic Considerations and Theory of Volume Change." *Journal of Applied Chemistry,* 14 (1964), 93-104.

[7] Helmuth, R.A. "Dimensional Changes and Water Adsorption of Hydrated Portland Cement and Tricalcium Silicate." *M.Sc. Thesis.* Chicago Institute of Technology, (1965).

[8] Wittman, R.H. "Interaction of Hardened Cement Paste and Water." *Journal of American Ceramic Society,* 56, No. 8 (1973), pp. 409-415.

[9] Parrott, L.J. and Young, J.F. "Shrinkage and Swelling of Two Hydrated Alite Pastes." *Int. Symp. on Fundamental Res. on Creep and Shrinkage of Concrete,* by Martinus Nijhoff Publishers (1982), 35-48.

[10] Feldman, R.F. and Sereda, P.J. "A Model for Hydrated Portland Cement and its Practical Implications." *Journal of Engineering,* 53, No. 8,9 (1970), 53-59.

[11] Young, J.F.; Berger, R.L. and Bentur, A. "Shrinkage of Tricalcium Silicate Pastes: Superposition of Several Mechanisms." *Cemento,* 75, No. 3 (1972), 391-398.

[12] Feldman, R.F. and Sereda, P.J. "A Model for Hydrated Portland Cement as Deduced from Sorption Length Changes and Mechanical Properties." *Mater. and Struct.,* 1, No. 1 (1968), 509-520.

[13] Bazant, Z.P. "Thermodynamics of Hindered Adsorption and its Implications for Hardened Cement and Concrete." *Cem. Conc. Res.,* 2, No. 1 (1972), 1-16.

[14] Wittman, F.H. "The Structure of Hardened Cement Paste-A Basic for a Better Understanding of the Materials Properties." *Cem. Conc. Assoc.,* London, England (1976), 96-117.

[15] Ishai, O. "The Time-Department Deformational Behaviour of Cement Paste, Mortar and Concrete." *Proc. Conf. Structure of Concrete and Its Behaviour Under Load,* Cement and Concrete Association, London (1968), 345-364.

[16] Hansen, W. "Investigation of Shrinkage Mechanisms in Hydrated and Carbonated Tricalcium Silicate System." *Ph.D. Thesis,* University of Illinois, (1983).

[17] Litvan, G.G. "Variability of the Nitrogen Surface Area of Hydrated Cement Paste." *Cem. Conc. Res.* 6 (1976), 139-144.

[18] Day, R.L. "Relations Between Methanol and Portland Cement Paste." *Cement and Concrete Research,* 11, No. 3 (1981), 341-349.

[19] Parrott, L. "Measurement and Modeling of Porosity in Drying Cement Paste, Symp. Proc. Materials Research Society." *Microstructural Development During Hydration of Cement,* 85 (1987), 91-104.

[20] Cranston, R.W. and Inkley, F.A. "The Determination of Pore Structures from Nitrogen Adsorption Isotherms." *Advances in Catalysis,* 9 (1957), 143-154.

[21] Bangham, D.H. and Fakhoury, N. "The Swelling of Charcoal. I Preliminary Experiments with Water Vapor, Carbon Dioxide, Ammonia and Sulphur Dioxide." *Proc. of the Royal Society,* London, Series A, 135 (1930), 81-89.

[22] Bangham, D.H.; Fakhoury, N. and Mohamed, A.F. "The Swelling of Charcoal, II. Some Factors Controlling the Expansion Caused by Water, Benzene and Pyridine Vapors." *Proc. Royal Society,* London, Series A (1932), 138-162.

[23] Amberg, C.H. and MacIntosh, R. "A Study of Adsorption Hysteresis by Means of Length Changes of a Rod of Porous Glass." *Canadian Journal of Chemistry,* 30 (1952), 1012-1032.

[24] Bangham, D.H. and Maggs, F.A. "The Strength and Elastic Constant of Coal in Relation to their Ultrafine Structure." *Proceedings of a Conference on the Ultrafine Structure of Coals and Cokes,* British Coal Utilization Research Association Committee, London (1943), 118-130.

[25] Hiller, K.H. "Strength Reduction of Length Changes in Porous Glass Caused by Water Vapor Adsorption." *Journal of Applied Physics,* 35, No. 5, (1964), 1622-1628.

[26] Yates, D.J.C. "Molecular Specificity in Physical Adsorption." *Advances in Catalysis.* 12 (1960), 265-311.

[27] Hwang, C.L. "Drying Shrinkage and Microstructure of Hydrated Cement Paste." *Ph.D Thesis,* University of Illinois (1983).

[28] Hobbs, D.W. and Mears, A.R. "The Influence of Specimen Geometry upon Weight Change and Shrinkage of Air-Dried Mortar Specimens." *Magazine of Concrete Research,* 23, No. 75, 76 (1971), 89-98.

[29] L'Hermite, R.A. and Mamillan, M. "Further Results of Shrinkage and Creep Test." *Inter. Confer. on the Struct. of Conc.,* Cem. and Conc. Assoc., London (1965), 423-433.

[30] Helmuth, R.A. and Turk, D.H. "The Reversible and Irreversible Drying Shrinkage of Hardened Portland Cement and Tricalcium Silicate Paste." *Journal PCA Res. Dev. Lab.* 9, No. 2 (1967), 8-21.

[31] Parrott, L.J.; Hansen, W. and Berger, R.L. "Effect of Drying and Rewetting Upon the Pore Structure of Hydrate Alite Paste." *Cem. Conc. Res.,* 10, No. 5 (1980), 647-655.

تقدير نسبة التغير في طول العجينة الأسمنتية البورتلاندية: تأثير العوامل الميكانيكية على هذا التغير

جمال عبدالرزاق سليمان المديهيم

أستاذ مساعد، قسم الهندسة المدنية، كلية الهندسة، جامعة الملك سعود، ص.ب ٨٠٠، الرياض ١١٤٢١، المملكة العربية السعودية

ملخص البحث. تمت دراسة تغير طول عجينة الأسمنت نتيجة التجفيف من ناحية علاقته بالمؤثرين الميكانيكيين (جبس بانجهام والإجهاد الشعري).

كما تمت قياسات تغير الطول إضافة إلى قابلية امتصاص النتروجين لعينات لها نسبة ماء إلى أسمنت قدره ٠,٤، ٠,٦، ٠,٧٥. وقيس مقدار تأثير كل نوع من الأنواع الميكانيكية على التغير بالطول من علاقة تغير الطول مع جهد السطح الحر في حدود نسبة رطوبة ما بين ٩٥٪ إلى صفر٪. لقد وجد أن المؤثر الميكانيكي الأول له أثر كبير جدا في عملية توليد إجهادات على العجينة الأسمنتية في حدود نسبة الرطوبة الموضحة. بينما المؤثر الميكانيكي الثاني يؤثر فقط في حدود نسبة رطوبة ما بين ٩٥٪ إلى ٥٠٪. كما لوحظ أن أكبر قيم التغير نتيجة للإجهاد من المؤثر الأول (وهي عند نسبة رطوبة صفر٪) تتناسب طرديا مع المساحة الكلية الداخلية للفراغات والمحسوبة من منحنى الحجم مع سمك الطبقة الممتصة. كذلك فإن أكبر قيم التغير الحاصل نتيجة للإجهاد من المؤثر الثاني (وهي عند نسبة رطوبة ٥٠٪) تتناسب طرديا مع مساحة الفراغات الشعرية الداخلية والمحسوبة من منحنى الحجم مع سمك الطبقة الممتصة. هذه العلاقات تم تحسينها لكي تأخذ بالاعتبار تأثير نسبة الرطوبة على تغير الطول. في النهاية تم فحص هذه العلاقات على معلومات تتعلق بتغير العجينة الأسمنتية التي تحتوي على نسب مختلفة من الماء إلى الأسمنت ووجد بأن هذه العلاقات جيدة.